Raman profiles of the stratum corneum define 3 filaggrin genotype–determined atopic dermatitis endophenotypes

Gráinne M. O'Regan, MRCPI,[a,b] Patrick M. J. H. Kemperman, MD,[c] Aileen Sandilands, PhD,[d] Huijia Chen, MD,[d] Linda E. Campbell, BSc,[d] Karin Kroboth, PhD,[d] Rosemarie Watson, MD,[b] Marion Rowland, MB, PhD,[a,e] Gerwin J. Puppels, PhD,[f,g] W. H. Irwin McLean, DSc, FMedSci,[d] Peter J. Caspers, PhD,[f,g]* and Alan D. Irvine, MD, FRCPI[a,b,h]*   *Dublin, Ireland, Rotterdam, The Netherlands, and Dundee, United Kingdom*

Background: Filaggrin (*FLG*) has a central role in the pathogenesis of atopic dermatitis (AD). *FLG* is a complex repetitive gene; highly population-specific mutations and multiple rare mutations make routine genotyping complex. Furthermore, the mechanistic pathways through which mutations in *FLG* predispose to AD are unclear.

Objectives: We sought to determine whether specific Raman microspectroscopic natural moisturizing factor (NMF) signatures of the stratum corneum could be used as markers of *FLG* genotype in patients with moderate-to-severe AD.

Methods: The composition and function of the stratum corneum in 132 well-characterized patients with moderate-to-severe AD were assessed by means of confocal Raman microspectroscopy and measurement of transepidermal water loss (TEWL). These parameters were compared with *FLG* genotype and clinical assessment.

Results: Three subpopulations closely corresponding with *FLG* genotype were identified by using Raman spectroscopy. The Raman signature of NMF discriminated between *FLG*-associated AD and non–*FLG*-associated AD (area under the curve, 0.94; 95% CI, 0.91-0.99). In addition, within the subset of *FLG*-associated AD, NMF distinguished between patients with 1 versus 2 mutations. Five novel *FLG* mutations were found on rescreening outlying patients with Raman signatures suggestive of undetected mutations (R3418X, G1138X, S1040X, 10085delC, and L2933X). TEWL did not associate with *FLG* genotype subgroups.

Conclusions: Raman spectroscopy permits rapid and highly accurate stratification of *FLG*-associated AD. *FLG* mutations do not influence TEWL within established moderate-to-severe AD. (J Allergy Clin Immunol 2010;126:574-80.)

Key words: Atopic dermatitis, confocal Raman spectroscopy, eczema, filaggrin, hyperlinearity, natural moisturizing factor, transepidermal water loss, tyrosine

Discuss this article on the JACI Journal Club blog: www.jaci-online.blogspot.com.

Atopic dermatitis (AD) is a complex and heterogeneous inflammatory skin disease driven and modified by immunologic, environmental, and genetic factors.[1,2] The identification of filaggrin (*FLG*) null alleles in up to 50% of patients with moderate-to-severe AD implicates a fundamental role for barrier homeostasis in this disease.[3-6] Although the mechanisms leading to AD in *FLG* mutation carriers are unclear, the deficiency of *FLG* likely facilitates permeability of biologically active allergens and microbial colonization that subsequently trigger inflammatory cascades.[7] The recent identification of a murine model for *FLG* deficiency, with the detection of a homozygous frameshift mutation in the *Flg* gene in *flaky tail* mice, should accelerate our understanding of pathogenic mechanisms and therapeutic intervention points in patients with AD.[8]

Knowledge of the biochemical functions of filaggrin and its breakdown products indicate that a quantitative variation in gene or protein dosage might be relevant in determining phenotype.[9,10] Filaggrin is initially produced as profilaggrin, a large, insoluble, heavily phosphorylated protein consisting of 10 to 12 tandem repeats of filaggrin units separated by short hydrophobic linker peptides.[11,12] In the transitional layer profilaggrin is dephosphorylated and proteolytically processed into its functional filaggrin units, which bind to and collapse the keratin cytoskeleton and other intermediate filaments, acting as a scaffold for the subsequent reinforcement steps of the stratum corneum (SC).[13-15] Subsequently, filaggrin is progressively degraded within the SC into a pool of hygroscopic amino acids, including pyrrolidone carboxylic acid, urocanic acid, and alanine. This composite mixture of amino acids and their derivatives, together with specific salts and sugars, form the natural moisturizing factor (NMF).[16,17]

NMF is highly hygroscopic and plays a central role in maintaining hydration of the SC and is additionally proposed to have a significant role in maintenance of the pH gradient of the skin, cutaneous antimicrobial defense, and regulation of key

enzymatic events in the SC.[18,19] Filaggrin thus has complex functions, with roles in establishing structural and chemical barrier function, hydration, and maintenance of epidermal homeostasis in the face of continuous transformation.[20] Expression of filaggrin and subsequent breakdown of filaggrin into NMF is additionally determined based on properties of the microenvironment, including local pH, relative humidity, and protease activity.[17,21,22] *In vitro* evidence also indicates that filaggrin skin expression might be modulated by the atopic inflammatory response mediated by the cytokines IL-4 and IL-13.[23] Genetically determined modifiers of protein dosage include the copy number of filaggrin repeat units, which vary in the population from 10 to 12 units and segregate by normal Mendelian genetic mechanisms.[11,24] These genetic polymorphisms reflect tandem duplications of *FLG* repeats 8, 10, or both and might be an additional modifier of disease phenotype in heterozygotes who carry longer-sized variants on the unaffected allele.[25] Our early data suggest that NMF levels correlate with *FLG*-null allele status and might therefore directly contribute to the dry skin phenotype seen in both patients with ichthyosis vulgaris and those with AD.[10]

Raman spectroscopy is capable of measuring *in vivo* information regarding the molecular composition of the skin, including quantitative analysis of amino acids and water content. It is based on the inelastic light scattering, or Raman scattering, of monochromatic light when the frequency of photons, usually from a laser source, changes on interaction with a sample, giving rise to characteristic Raman spectra and providing noninvasive real-time signatures of biological samples at a molecular level.

We sought to determine whether specific Raman NMF signatures of the SC could be used as markers of *FLG* genotype in patients with moderate-to-severe AD. We examined the association of NMF estimation with clinical evidence of hyperlinear palms (HLP), a clinical sign that has been shown to be associated with *FLG* mutations in previous studies. We also sought to examine the effects, within patients with moderate-to-severe AD, of *FLG* genotype on transepidermal water loss (TEWL) as a measure of an inside-out barrier defect.

METHODS

Following standard genetic practice, in this article $FLG^{-/-}$ designates a patient homozygous for null alleles (ie, 2 null alleles), $FLG^{+/-}$ designates a heterozygote null allele/wild-type (ie, 1 null allele), and $FLG^{+/+}$ designates a homozygous wild-type (ie, 0 null alleles). A further abbreviation describes patients with AD with *FLG* mutations ($FLG^{+/-}$ and $FLG^{-/-}$) as AD_{FLG} and those without *FLG* mutations (ie, $FLG^{+/+}$) as $AD_{NON-FLG}$.

One hundred thirty-five unrelated Irish children with a history of moderate-to-severe AD were recruited from dedicated tertiary referral AD clinics. Diagnosis was made by experienced pediatric dermatologists according to the United Kingdom diagnostic criteria.[26] Exclusion criteria from the study were patients who had received systemic therapy, such as corticosteroids or immunosuppressants, in the preceding 3 months and patients whose ancestry was not exclusively Irish (4/4 grandparents). Detailed phenotypic data were collected. The Nottingham Eczema Severity Score[27] was selected as an estimate of disease severity. Given previous publications and our own clinical experience of noting palmar hyperlinearity, this clinical sign was scored by using an investigator assessment of 0 (no hyperlinearity), 1 (mild/subtle hyperlinearity), and 2 (severe hyperlinearity).

Genetic screening

All patients were screened for the 6 most prevalent *FLG* mutations in the Irish population (R501X, 2282del4, R2447X, S3247X, 3702delG, and Y2092X), as previously described.[28] Full sequencing of *FLG* was performed as detailed previously.[28] Based on screening for these 6 prevalent *FLG* mutations, 58.3% were carriers of 1 or more *FLG* mutations (15.1% $FLG^{-/-}$, 43.2% $FLG^{+/-}$, and 41.7% $FLG^{+/+}$). An additional rare mutation was known to be present in 1 subject in a heterozygous state (R1474X). Additional screening was performed by means of complete sequencing of the *FLG* gene in selected subjects, as previously described.[29] The entire collection was then rescreened for these 5 novel mutations found on complete sequencing.

Biophysical analysis of the SC

Skin biophysical measurements were performed under standardized conditions (room temperature, 22°C-25°C; humidity levels, 30% to 35%). Before measurements, patients were acclimatized for a minimum of 10 minutes. All measurements were performed by one of 2 investigators (G.M.O. and P.M.J.H.K.). Topical therapies, including emollients, were withheld from the measurement sites for 48 hours preceding the study. TEWL was measured on nonlesional skin of the extensor forearm (Tewameter 300; Courage and Khazaka Electronic GmbH, Cologne, Germany).

NMF was measured in the SC of the thenar eminence by using confocal Raman microspectroscopy (model 3510 Skin Composition Analyzer; River Diagnostics, Rotterdam, The Netherlands). The principles of this method and the procedure have been described elsewhere.[30,31] Depth profiles of Raman spectra were measured at 5-μm intervals from the skin surface at 30, 35, 40, 45 and 50 μm below the skin surface. An average of 8 profiles (totaling to 40 Raman spectra) from different areas of the thenar eminence were measured per patient. Raman spectra were recorded in the spectral region at 400 to 1,800 cm^{-1} with a 785-nm laser. Laser power on the skin was 25 mW. Levels of skin constituents relative to keratin were determined from the Raman spectra by means of classical least-squares fitting. Details of the method have been described elsewhere.[30,31] Briefly, reference spectra of keratin, NMF, urocanic acid, lactate, urea, ceramide, and cholesterol were fitted to the individual Raman spectra from the skin. The combination of these reference spectra provides an adequate model for *in vivo* Raman spectra of normal human SC. A spectrum of reagent-grade L-tyrosine (Sigma-Aldrich, Zwijndrecht, The Netherlands) was added to this set of reference-fit spectra to enable determination of increased tyrosine levels. The resulting fit coefficients represent the relative proportions in which the skin constituents contribute to the total Raman skin spectrum. The reference spectrum of NMF had been constructed from the weighted sum of the spectra of its dominant constituents (pyrrolidone carboxylic acid, ornithine, serine, proline, glycine, histidine, and alanine). All concentrations of skin constituents relative to keratin were calculated from the recorded Raman spectra by using SkinTools 2.0 (River Diagnostics B.V., Rotterdam, The Netherlands); NMF levels derived from the individual Raman spectra were used to assess intrapatient variation in NMF. These NMF levels were then averaged to obtain the mean NMF level per patient. Of the 135 subjects who participated in the study, 3 patients were unable to fully cooperate with the Raman measurement, and their results were excluded because of insufficient spectra collection.

The study was conducted in accordance with the Declaration of Helsinki and was approved by the Research Ethics Committee of Our Lady's Children's Hospital, Dublin. Written informed consent was obtained from all patients or their parents.

Statistical methods

Patients were characterized, *a priori*, into 3 genotypes ($FLG^{+/+}$, $FLG^{+/-}$, and $FLG^{-/-}$), as described in the methods. The designation *FLG-associated*

AD (AD_{FLG}) includes those with 1 or 2 *FLG* mutations ($FLG^{+/-}$ and $FLG^{-/-}$), whereas non–*FLG*-associated AD ($AD_{NON-FLG}$) are $FLG^{+/+}$. The data were characterized as having either a normal or a skewed distribution. Positively skewed data were log transformed. Box and whiskers plots showing the median value with interquartile range (25th-75th box length) of variables were constructed for the 3 *FLG* genotypes ($FLG^{-/-}$, $FLG^{+/-}$, and $FLG^{+/+}$). ANOVA was used to compare means among the 3 genotype subgroups and presented as means with SDs and 95% CIs. Homogeneity of variances was tested by using the Levine statistic. A *post hoc* Tukey analysis for multiple comparisons was performed to examine pairwise differences among the 3 genotype subgroups. Mean differences for each pairwise comparison was presented together with a 95% CI of the mean difference.

Nonparametric receiver operating characteristic (ROC) curves, which plot sensitivity against 1−specificity, were constructed to examine the utility of Raman spectroscopy to, in the first instance, differentiate between AD_{FLG} and $AD_{NON-FLG}$. We then sought to further determine whether, within the *FLG*-associated AD group, ROC curve analysis could determine an NMF cutoff point to predict homozygous or heterozygous subjects ($FLG^{-/-}$ vs $FLG^{+/-}$). Areas under the curve (AUCs) with 95% CIs are presented. The cutoff for maximal sensitivity and specificity was deduced from the graphic output. Sensitivity and specificity for our dataset, based on the ROC output, are also presented to provide a preliminary indication of the clinical utility of Raman spectroscopy as a novel technique to distinguish *FLG* genotypes in patients with AD. However, further evaluation of Raman spectroscopy will be required in different well-characterized populations of patients with AD and healthy subjects.

HLP was scored clinically as absent (0) mild (1), or severe (2). For statistical analysis, HLP was dichotomized to no evidence of hyperlinearity (clinical score 0) versus any hyperlinearity (clinical scores of 1 or 2). The κ statistic was used to measure agreement between clinical scores of HLP and an NMF cutoff of 1.07. Where the observed agreement between scores is better than the degree of agreement expected by chance alone, κ is scored from 0 to 1.0, with 1.0 representing perfect agreement. A κ value of less than 0.2 is poor, a score of 0.2 to 0.4 is fair, 0.4 to 0.6 is considered moderate agreement, 0.6 to 0.8 is considered good agreement, and greater than 0.8 is considered excellent agreement.[32] Data were analyzed with SPSS software (version 15; SPSS, Inc, Chicago, Ill). Significance was set at the 5% level.

RESULTS

Clinical characteristics and summary data of the study cohort are outlined in Table I. NMF levels assessed by means of Raman spectroscopy for subjects according to final *FLG* genotype (final genotype after full screening) are shown in Fig 1. In each pairwise comparison of the 3 genotypes, there is a statistically significant difference in NMF values ($P < .001$, ANOVA, Tukey post hoc analysis; Table II). IgE levels were not normally distributed. After log transformation of IgE data, there was no statistically significant difference in IgE values among the 3 *FLG* mutation subgroups ($P < .48$, Table I).

Within the $FLG^{+/+}$ and $FLG^{+/-}$ genotype subgroups, 13 subjects had significantly outlying values with significantly lower NMF values compared with others who shared these genotypes (Fig 2). We hypothesized that these outlying values were suggestive of additional undetected *FLG* mutations. These 13 subjects were therefore fully sequenced for potential additional mutations. After full sequencing of these 13 subjects, 5 novel mutations (R3418X, G1138X, S1040X, 10085delC and L2933X) were detected. The entire collection was then rescreened to include 11 mutations (6 on initial screening plus these 5 additional mutations); however, no additional patients were found to harbor these novel rare mutations. NMF values by genotype after this additional screening are plotted in histogram format in Fig 3. Within *FLG* genotype subgroups, a range of values was seen; these values approximate to a normal distribution in each of the 3 genotype subgroups. The new mutations increased the percentage of patients with 1 or more *FLG* mutations in the collection to 59.8% (18.2% $FLG^{-/-}$, 41.7% $FLG^{+/-}$, and 40.2% $FLG^{+/+}$; Table I).

NMF values predict *FLG* genotype in patients with moderate-to-severe AD

ROC curves were constructed to examine the discriminatory power of Raman-determined NMF. From a clinical decision tree, patients were initially grouped as AD_{FLG} and $AD_{NON-FLG}$ ($FLG^{+/+}$). The discriminatory power of Raman-determined NMF here was high, with an AUC on ROC analysis of 0.95 (95% CI, 0.91-0.99; Fig 4). The optimal cutoff value for NMF was 1.07, which would equate to a sensitivity of 98.73% and a specificity of 86.89% extrapolated from our ROC analysis. With the AD_{FLG} group of children, NMF values also distinguished between $FLG^{+/-}$ and $FLG^{-/-}$ subjects, with an ROC AUC of 0.85 (95% CI, 0.77-0.93; see Fig E1 in this article's Online Repository at www.jacionline.org). This sensitivity and specificity is presented to suggest the probable utility of Raman spectroscopy as a novel diagnostic technique in patients with AD and is not presented as a test for the goodness of fit of the model.

Tyrosine peaks on Raman microspectroscopy predict $FLG^{-/-}$ genotype

The Raman spectra collected in the study revealed a distinct signal profile in a subset of patients subsequently identified by matching of *in vitro* Raman spectra of the amino acid tyrosine. Tyrosine levels 5 SDs greater than the normal tyrosine level measured in $FLG^{+/+}$ subjects were identified as increased. Above this threshold, distinct tyrosine peaks could be visually identified in the corresponding Raman spectra. Tyrosine peaks were present in 19 (79%) of 24 of the patients who had 2 *FLG* mutations (Table I) and absent from all but 1 $FLG^{+/+}$ subject, who also had an outlying low NMF level (Fig 5), suggesting an undetected genetic defect in *FLG*. The optimum NMF cutoff to correlate with tyrosine peaks was 0.831 (AUC, 0.81; 95% CI, 0.73-0.89), which is similar to the cutoff that distinguishes the $FLG^{-/-}$ from the $FLG^{+/-}$ populations (data not shown).

TEWL in patients with moderate-to-severe AD does not discriminate between *FLG* genotype subgroups

There was no difference in mean TEWL levels among the 3 *FLG* genotype subgroups (Table I). TEWL did not distinguish *FLG* genotype status in patients with AD (TEWL AUC, 0.583; 95% CI, 0.48-0.699; ROC curve not shown).

NMF values and palmar hyperlinearity scores

There was good agreement between clinical assessment of palmar hyperlinearity and an NMF cutoff of 1.07 (κ = 0.71). Thus palmar hyperlinearity might help distinguish patients with AD into those with 1 or more *FLG* mutations versus those with none. Clinical assessment is not as accurate as Raman spectroscopy in distinguishing the 3 *FLG* genotypes. The Nottingham Eczema Severity Score did not segregate with *FLG* genotype in this collection (data not shown), suggesting that the spectrum of AD severity within this moderate-to-severe collection is independent of *FLG* genotype.

TABLE I. Cohort characteristics according to final genotype

Final *FLG* genotype*†	All mutations combined, no. (%)	Age (y), mean (SD)	Male sex, no. (%)	NESS,‡ mean (SD)	Palmar hyperlinearity score‡	TEWL (g/m²/h), mean (SD)	NMF (AU), mean (SD)	Tyrosine peaks, no. (%)	Log IgE# mean (SD)
Screened§	n = 132	n = 132	n = 132	n = 132	n = 131	n = 102	n = 132	n = 132	n = 129
+/+	53 (40.15)	8.43 (3.76)	32 (60.3)	12.40 (2.39)	0: 36	15.54 (9.34), n = 41	1.31 (0.24)	1 (1.89)	6.89 (2.29)
					1: 10				
					2: 7				
					n = 53				
+/−	55 (41.66)	8.2 (4.12)	32 (58.2)	11.28 (2.80)	0: 8	15.59 (6.72), n = 44	0.80 (0.21)	10 (18.18)	6.56 (1.78)
					1: 23				
					2: 23				
					n = 54				
−/−	24 (18.18)	8.83 (4.16)	15 (62.5)	12.13 (2.52)	0: 0	17.35 (7.37), n = 17	0.57 (0.15)	19 (79.16)	7.11 (1.50)
					1: 1				
					2: 23				
					n=24				
P value	−	.84‖	.97¶	.07‖	−	.70‖	<.0001‖	<.0001¶	.48‖

AU, Arbitrary units.

*Final *FLG* status after rescreening cohort for all mutations (*FLG* status before detection of novel mutations: $FLG^{+/+}$, 41.7%; $FLG^{+/−}$, 43.2%; and $FLG^{−/−}$, 15.1%).

†+/+, No *FLG* mutation; +/−, 1 *FLG* mutation; −/−, 2 *FLG* mutations.

‡*NESS*, Nottingham Eczema Severity Score. Palmar hyperlinearity score: 0, no hyperlinearity; 1, intermediate; 2, marked.

§Hyperlinearity scoring and TEWL data are not available for 1 and 30 subjects, respectively.

‖Comparison of means among the 3 groups of *FLG* mutations using ANOVA.

¶Comparison of proportions using χ^2 test for comparison of a 2 × 3 contingency table.

#IgE data were positively skewed. The mean of the log-transformed data is presented.

DISCUSSION

A primary aim of this study was to investigate the utility of *in vivo* measurements of the SC to differentiate between *FLG* genotypes within patients with AD. Second, by making use of a very well-genotyped collection, we sought to determine whether *FLG* genotype influenced TEWL in patients with established moderate-to-severe AD. These results establish that the biochemical composition of the SC and palmar hyperlinearity associate with *FLG* mutation status, allowing rapid stratification of AD endotypes. Furthermore, we conclude that the degree of barrier defect, as measured by TEWL, in the clinically unaffected skin of patients with established AD is not influenced by *FLG* genotype.

The clinical utility of Raman-determined NMF is powerfully illustrated in the ROC curve analysis, which has an AUC of 0.95 (95% CI, 0.91-0.99) to discriminate between the AD_{FLG} and $AD_{NON-FLG}$ groups. In addition, NMF can distinguish from heterozygous *FLG* mutations. In other words, this technique allows segregation of AD into *FLG* genotypes (+/+, +/−, and −/−) with such high specificity that it can accurately predict *FLG* genotype. Even in this relatively small patient population, mean NMF was statistically different between each of the 3 subpopulations (*post hoc* Tukey, Table II) Further validation of Raman-determined NMF is required in patients with well-characterized AD and healthy populations before this novel technique can be considered for clinical use.

The observed interindividual variation in NMF results within the mutation groups approximates to a normal distribution (Fig 3) that might be caused by environmental, genetic, or immunologic modifiers of *FLG* expression, including posttranslational processing. Homeostatic mechanisms or genetic mechanisms, such as the effects of copy number variation, small gene deletions, cytokine modulation of *FLG* expression, or upregulation of additional sources of NMF constituents, such as eccrine-derived lactate and glycerol, might account for differences in NMF levels within genotype groups. Modifying genes involved in filaggrin-processing pathways are likely to additionally contribute to this
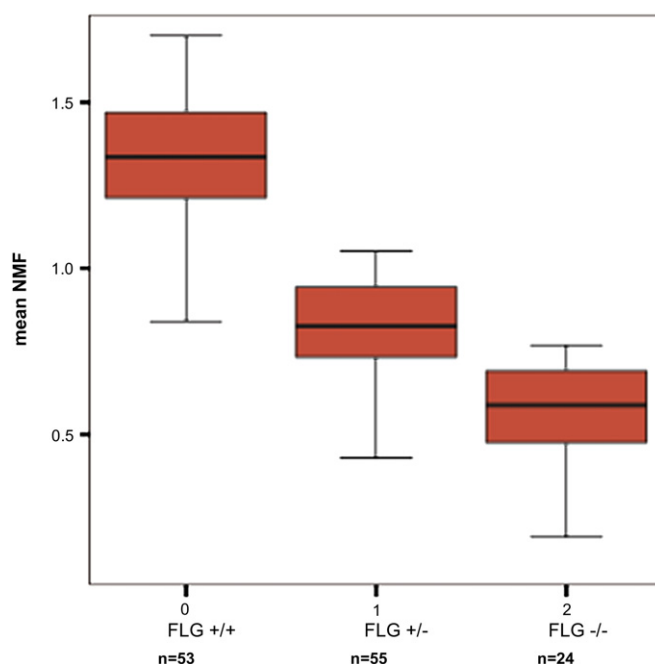

FIG 1. Box and whiskers plot of NMF by *FLG* genotypes (final genotype after full screening) showing the median *(midline)* and interquartile range corresponding to the length of the box.

variation.[20] The strong relationship between *FLG* mutation status and NMF implies that the role of other histidine-rich barrier proteins, such as the S100-fused proteins, including filaggrin-2 and hornerin, that are thought to have synergistic roles with filaggrin, including contribution to NMF levels,[33-35] are unlikely to play a major role in the total NMF seen in AD patients.
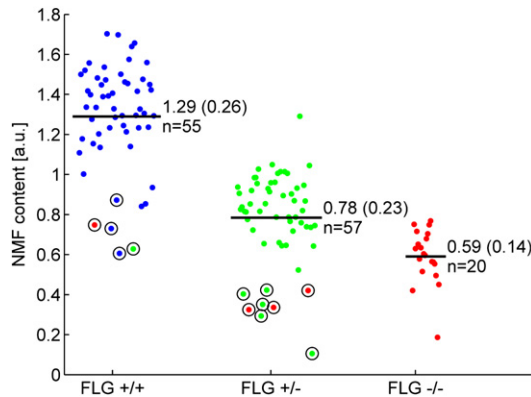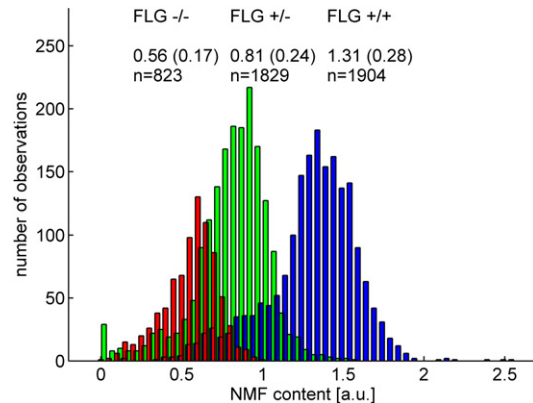
The strong predictive value of a tyrosine signal in the SC of subjects with *FLG* mutations identifies a potential biomarker in

TABLE II. ANOVA showing a statistically significant difference in NMF among the 3 *FLG* genotype subgroups together with 95% CIs

Genotype	No.	Mean NMF	95% CI	Comparison genotype	Mean difference	95% CI mean difference	P value*
$FLG^{+/+}$	53	1.31 ± 0.24	1.24 to 1.37	$FLG^{+/-}$	0.51	0.40 to 0.60	<.001
				$FLG^{-/-}$	0.74	0.62 to 0.87	<.001
$FLG^{+/-}$	55	0.80 ± 0.21	0.74 to 0.86	$FLG^{+/+}$	−0.51	−0.60- to −0.41	<.001
				$FLG^{-/-}$	0.24	0.11 to 0.36	<.001
$FLG^{-/-}$	24	0.57 ± 0.15	0.50 to 0.63	$FLG^{+/+}$	−0.74	−8.86 to −0.61	<.001
				$FLG^{+/-}$	−0.24	−0.36 to −0.11	<.001

A *post hoc* analysis with Tukey correction shows a statistically significant difference in mean NMF between each pairwise comparison for the 3 *FLG* genotype subgroups.
*Tukey multiple comparisons.

FIG 2. NMF cloud plot of values subcategorized after initial screening of 6 prevalent mutations. *Circles* indicate outliers who were rescreened for additional mutations. *Colors* indicate the final genotype after full screening. For each group, the number of patients and average NMF level (mean ± SD) are indicated in the figure. Group comparisons showing means and standard deviations by using ANOVA are presented in the text. *a.u.*, Arbitrary units.

FIG 3. Histogram of all nonaveraged NMF values subcategorized according to corrected mutational status. *Blue bars* are $FLG^{+/+}$ subjects, *green bars* are $FLG^{+/-}$ subjects, and *red bars* are $FLG^{-/-}$ subjects. For each group, the number of Raman measurements and the average NMF level (mean ± SD) are indicated in the figure. *FLG* genotype group sizes are as follows: $FLG^{-/-}$, 24; $FLG^{+/-}$, 55; $FLG^{+/+}$, 53. *a.u.*, Arbitrary units.

the diagnosis of *FLG*-null subjects. Filaggrin lacks tyrosine; however, the linker segments and carboxyl-terminal domains of profilaggrin contain dense and highly conserved tyrosine-rich motifs.[11,12,36] In normal SC only tyrosine incorporated in proteins, predominantly keratin, contributes to the overall Raman spectrum of skin; unbound tyrosine is usually not detectable. The consistent observation of the presence of tyrosine peaks in homozygous *FLG* mutation carriers might relate to altered biosynthetic pathways, such as limited proteolysis of profilaggrin or aberrant intermediate processing species, degraded through alternative pathways. The presence of tyrosine is independent of disease severity or mutation location.

Palmar and plantar hyperlinearity is a consistent clinical finding in the monogenic *FLG* disease ichthyosis vulgaris, and in keeping with a semidominant trait, intermediate hyperlinearity is thought to be associated with heterozygosity for *FLG* mutations; hyperlinearity has been associated as a significant finding in patients with *FLG*-related AD.[37-40] Brown et al[41] have recently shown significant association of palmar hyperlinearity with *FLG*-null mutations in a population-based cohort.[41] Our finding that *FLG* status and NMF segregate with palmar hyperlinearity in patients with moderate-to-severe AD further validates the importance of this clinical sign in AD phenotypes.

Evidence from both molecular genetics and functional analyses strongly supports a skin barrier defect as a feature of both lesional and nonlesional skin in patients with AD.[42-44] Increased mean baseline TEWL levels, reflecting a dysfunction of the inside-out

epidermal permeability barrier in the clinically uninvolved skin of patients with AD, have been shown in many previous studies.[45-47] The concept of an inherent skin barrier defect in both lesional and nonlesional skin from patients with is further supported by other methodologies, including recent data by Jakasa et al[43] showing enhanced uptake of entire series of polyethylene glycols covering molecular weights in the range 150 to 590 daltons in nonlesional skin of patients with AD. Hata et al, using a photoacoustic spectroscopic system, showed enhanced penetration of both lipophilic and hydrophilic dye through clinically normal skin of patients with AD compared with that seen in control subjects.[42-44]

Previous investigators have reported contrasting findings on the influence of *FLG* mutation status on the inside-out barrier, as measured by TEWL in patients with AD; however, these studies were restricted by small sample size and possibly confounded by the technical limitations of disclosure of full *FLG* polymorphism status in the populations studied.[10,48] A French study including a small number of *FLG* mutation carriers suggested that TEWL in patients with AD was not influenced by *FLG* status.[49] Here, in our much larger collection of comprehensively genotyped patients with moderate-to-severe AD, TEWL again showed no discernable difference between *FLG* genotype subpopulations. These results suggest that increased TEWL in patients with moderate-to-severe AD is independent of *FLG* status and is a common end point in patients with moderate-to-severe AD. Thus increased TEWL might result from the systemic effects of the inflammatory
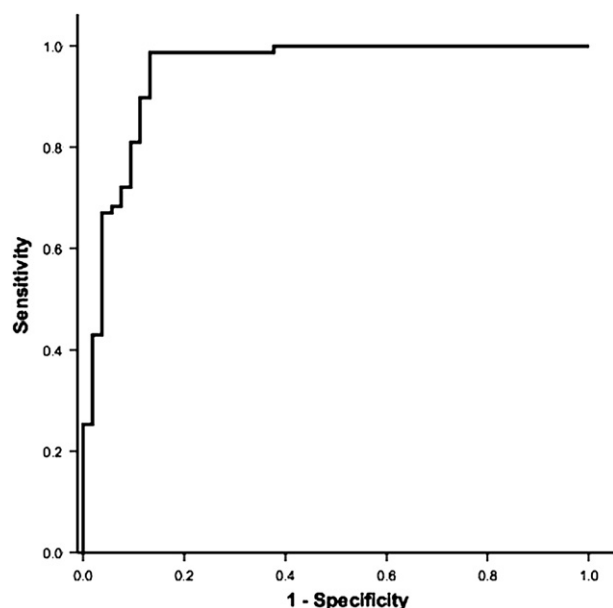
FIG 4. ROC curve for NMF AD$_{FLG}$ (genotype $+/-$ and $-/-$) compared with AD$_{NON\text{-}FLG}$ (genotype $+/+$). The AUC is 0.95 (95% CI, 0.91-0.99). The optimal cutoff point for mean NMF to distinguish AD$_{FLG}$ from AD$_{NON\text{-}FLG}$ was 1.07 arbitrary units.
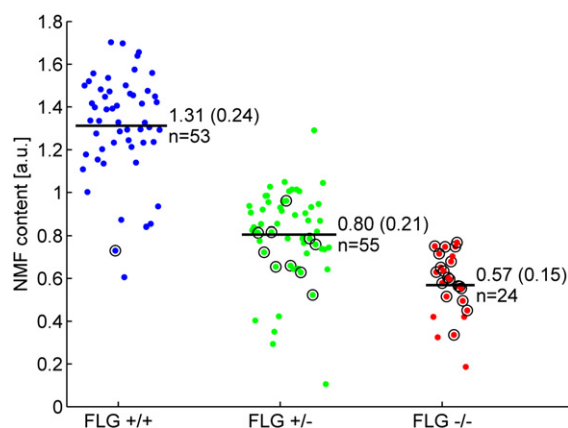

FIG 5. Cloud plot of NMF values categorized by genotype (final genotype after full screening). *Circles* indicate subjects with an increased tyrosine signal (*FLG*$^{+/+}$, n = 1; *FLG*$^{+/-}$, n = 10; *FLG*$^{-/-}$, n = 19). For each group, the number of patients and average NMF level (mean $\pm$ SD) are indicated in the figure. *a.u.*, Arbitrary units.

process, even at nonclinically inflamed sites. Interestingly, flaky tail *(ft)* mice show a moderate increase in baseline TEWL, a deviation that increases dramatically after allergen priming and the subsequent secondary inflammatory response.[8] In these mice, although *FLG* deficiency might of itself lead to an inside-out barrier defect barely measureable by increased TEWL, the subsequent marked increase in TEWL appears to be driven by the secondary immunologic response.

Within this collection, no effect was seen for *FLG* and disease severity or total serum IgE level; however, this case series is not the ideal collection to examine this because all cases are moderate to severe and therefore the full range of severity is not represented. Further population-based and sufficiently powered studies should clarify this potential genotype-phenotype correlation.

Within patients with AD, Raman signatures of NMF level and tyrosine predict *FLG* mutation status, overcoming the need for technically demanding genotyping, particularly in populations in which the *FLG* mutation architecture has not been comprehensively elucidated. This work additionally further informs mechanistic pathways in AD, demonstrating that TEWL in patients with moderate-to-severe AD is an outcome that is independent of *FLG* mutation status and pointing to a complex systemic interplay of environmental, immunologic, and functional pathways in the genesis of epithelial barrier disruption in patients with AD.

Key messages

- **Raman spectroscopy, specifically NMF analysis, permits rapid and accurate stratification of FLG-associated versus non–FLG-associated AD and might be useful as a predictive test for FLG mutations.**

- **There is good agreement between FLG mutation status, NMF, and clinical palmar hyperlinearity scoring in patients with moderate-to-severe AD. Palmar hyperlinearity might help to define a clinical and genetic phenotype of AD.**

- **Within patients with moderate-to-severe AD, TEWL levels do not segregate with FLG genotype, suggesting that FLG mutations are neither necessary nor sufficient to fully explain this inside-out barrier defect in established AD.**

REFERENCES

1. Bieber T. Atopic dermatitis. N Engl J Med 2008;358:1483-94.
2. Leung DY, Bieber T. Atopic dermatitis. Lancet 2003;361:151-60.
3. Sandilands A, O'Regan GM, Liao H, Zhao Y, Terron-Kwiatkowski A, Watson RM, et al. Prevalent and rare mutations in the gene encoding filaggrin cause ichthyosis vulgaris and predispose individuals to atopic dermatitis. J Invest Dermatol 2006; 126:1770-5.
4. Barker JN, Palmer CN, Zhao Y, Liao H, Hull PR, Lee SP, et al. Null mutations in the filaggrin gene (FLG) determine major susceptibility to early-onset atopic dermatitis that persists into adulthood. J Invest Dermatol 2007;127:564-7.
5. Baurecht H, Irvine AD, Novak N, Illig T, Buhler B, Ring J, et al. Toward a major risk factor for atopic eczema: meta-analysis of filaggrin polymorphism data. J Allergy Clin Immunol 2007;120:1406-12.
6. Weidinger S, O'Sullivan M, Illig T, Baurecht H, Depner M, Rodriguez E, et al. Filaggrin mutations, atopic eczema, hay fever, and asthma in children. J Allergy Clin Immunol 2008;121:1203-9, e1.
7. Elias PM. Skin barrier function. Curr Allergy Asthma Rep 2008;8:299-305.
8. Fallon PG, Sasaki T, Sandilands A, Campbell LE, Saunders SP, Mangan NE, et al. A homozygous frameshift mutation in the mouse Flg gene facilitates enhanced percutaneous allergen priming. Nat Genet 2009;41:602-8.
9. Ginger RS, Blachford S, Rowland J, Rowson M, Harding CR. Filaggrin repeat number polymorphism is associated with a dry skin phenotype. Arch Dermatol Res 2005;297:235-41.
10. Kezic S, Kemperman PM, Koster ES, de Jongh CM, Thio HB, Campbell LE, et al. Loss-of-function mutations in the filaggrin gene lead to reduced level of natural moisturizing factor in the stratum corneum. J Invest Dermatol 2008;128:2117-9.
11. Gan SQ, McBride OW, Idler WW, Markova N, Steinert PM. Organization, structure, and polymorphisms of the human profilaggrin gene. Biochemistry 1990;29: 9432-40.
12. Presland RB, Haydock PV, Fleckman P, Nirunsuksiri W, Dale BA. Characterization of the human epidermal profilaggrin gene. Genomic organization and identification of an S-100-like calcium binding domain at the amino terminus. J Biol Chem 1992; 267:23772-81.
13. Segre J. Complex redundancy to build a simple epidermal permeability barrier. Curr Opin Cell Biol 2003;15:776-82.

14. Kalinin AE, Kajava AV, Steinert PM. Epithelial barrier function: assembly and structural features of the cornified cell envelope. Bioessays 2002;24:789-800.

15. Candi E, Schmidt R, Melino G. The cornified envelope: a model of cell death in the skin. Nat Rev Mol Cell Biol 2005;6:328-40.

16. Rawlings AV, Scott IR, Harding CR, Bowser PA. Stratum corneum moisturization at the molecular level. J Invest Dermatol 1994;103:731-41.

17. Scott IR, Harding CR. Filaggrin breakdown to water binding compounds during development of the rat stratum corneum is controlled by the water activity of the environment. Dev Biol 1986;115:84-92.

18. Rawlings AV, Matts PJ. Stratum corneum moisturization at the molecular level: an update in relation to the dry skin cycle. J Invest Dermatol 2005;124:1099-110.

19. Krien PM, Kermici M. Evidence for the existence of a self-regulated enzymatic process within the human stratum corneum—an unexpected role for urocanic acid. J Invest Dermatol 2000;115:414-20.

20. Sandilands A, Sutherland C, Irvine AD, McLean WH. Filaggrin in the frontline: role in skin barrier function and disease. J Cell Sci 2009;122:1285-94.

21. Bouwstra JA, Groenink HW, Kempenaar JA, Romeijn SG, Ponec M. Water distribution and natural moisturizer factor content in human skin equivalents are regulated by environmental relative humidity. J Invest Dermatol 2008;128:378-88.

22. Nakagawa N, Sakai S, Matsumoto M, Yamada K, Nagano M, Yuki T, et al. Relationship between NMF (lactate and potassium) content and the physical properties of the stratum corneum in healthy subjects. J Invest Dermatol 2004;122:755-63.

23. Howell MD, Kim BE, Gao P, Grant AV, Boguniewicz M, Debenedetto A, et al. Cytokine modulation of atopic dermatitis filaggrin skin expression. J Allergy Clin Immunol 2007;120:150-5.

24. McKinley-Grant LJ, Idler WW, Bernstein IA, Parry DA, Cannizzaro L, Croce CM, et al. Characterization of a cDNA clone encoding human filaggrin and localization of the gene to chromosome region 1q21. Proc Natl Acad Sci U S A 1989;86:4848-52.

25. Wong KK, deLeeuw RJ, Dosanjh NS, Kimm LR, Cheng Z, Horsman DE, et al. A comprehensive analysis of common copy-number variations in the human genome. Am J Hum Genet 2007;80:91-104.

26. Williams HC, Burney PG, Hay RJ, Archer CB, Shipley MJ, Hunter JJ, et al. The U.K. Working Party's Diagnostic Criteria for Atopic Dermatitis. I. Derivation of a minimum set of discriminators for atopic dermatitis. Br J Dermatol 1994;131:383-96.

27. Emerson RM, Charman CR, Williams HC. The Nottingham Eczema Severity Score: preliminary refinement of the Rajka and Langeland grading. Br J Dermatol 2000;142:288-97.

28. Sandilands A, Smith FJ, Irvine AD, McLean WH. Filaggrin's fuller figure: a glimpse into the genetic architecture of atopic dermatitis. J Invest Dermatol 2007;127:1282-4.

29. Sandilands A, Terron-Kwiatkowski A, Hull PR, O'Regan GM, Clayton TH, Watson RM, et al. Comprehensive analysis of the gene encoding filaggrin uncovers prevalent and rare mutations in ichthyosis vulgaris and atopic eczema. Nat Genet 2007;39:650-4.

30. Caspers PJ, Lucassen GW, Carter EA, Bruining HA, Puppels GJ. In vivo confocal Raman microspectroscopy of the skin: noninvasive determination of molecular concentration profiles. J Invest Dermatol 2001;116:434-42.

31. Caspers PJ, Lucassen GW, Puppels GJ. Combined in vivo confocal Raman spectroscopy and confocal microscopy of human skin. Biophys J 2003;85:572-80.

32. Daly LE, Bourke G. Interpretation and uses of medical statistics. 5th ed. Oxford: Blackwell Scientific Press; 2000. p. 381-421.

33. Esparza-Gordillo J, Weidinger S, Folster-Holst R, Bauerfeind A, Ruschendorf F, Patone G, et al. A common variant on chromosome 11q13 is associated with atopic dermatitis. Nat Genet 2009;41:596-601.

34. Wu Z, Hansmann B, Meyer-Hoffert U, Glaser R, Schroder JM. Molecular identification and expression analysis of filaggrin-2, a member of the S100 fused-type protein family. PLoS One 2009;4:e5227.

35. Toulza E, Mattiuzzo NR, Galliano MF, Jonca N, Dossat C, Jacob D, et al. Large-scale identification of human genes implicated in epidermal barrier function. Genome Biol 2007;8:R107.

36. Resing KA, Walsh KA, Haugen-Scofield J, Dale BA. Identification of proteolytic cleavage sites in the conversion of profilaggrin to filaggrin in mammalian epidermis. J Biol Chem 1989;264:1837-45.

37. Smith FJ, Irvine AD, Terron-Kwiatkowski A, Sandilands A, Campbell LE, Zhao Y, et al. Loss-of-function mutations in the gene encoding filaggrin cause ichthyosis vulgaris. Nat Genet 2006;38:337-42.

38. Novak N, Baurecht H, Schafer T, Rodriguez E, Wagenpfeil S, Klopp N, et al. Loss-of-function mutations in the filaggrin gene and allergic contact sensitization to nickel. J Invest Dermatol 2008;128:1430-5.

39. Weidinger S, Illig T, Baurecht H, Irvine AD, Rodriguez E, Diaz-Lacava A, et al. Loss-of-function variations within the filaggrin gene predispose for atopic dermatitis with allergic sensitizations. J Allergy Clin Immunol 2006;118:214-9.

40. Sergeant A, Campbell LE, Hull PR, Porter M, Palmer CN, Smith FJ, et al. Heterozygous null alleles in filaggrin contribute to clinical dry skin in young adults and the elderly. J Invest Dermatol 2009;129:1042-5.

41. Brown SJ, Relton CL, Liao H, Zhao Y, Sandilands A, McLean WH, et al. Filaggrin haploinsufficiency is highly penetrant and is associated with increased severity of eczema: further delineation of the skin phenotype in a prospective epidemiological study of 792 school children. Br J Dermatol 2009;161:884-9.

42. Jakasa I, Verberk MM, Bunge AL, Kruse J, Kezic S. Increased permeability for polyethylene glycols through skin compromised by sodium lauryl sulphate. Exp Dermatol 2006;15:801-7.

43. Jakasa I, Verberk MM, Esposito M, Bos JD, Kezic S. Altered penetration of polyethylene glycols into uninvolved skin of atopic dermatitis patients. J Invest Dermatol 2007;127:129-34.

44. Hata M, Tokura Y, Takigawa M, Sato M, Shioya Y, Fujikura Y, et al. Assessment of epidermal barrier function by photoacoustic spectrometry in relation to its importance in the pathogenesis of atopic dermatitis. Lab Invest 2002;82:1451-61.

45. Seidenari S, Giusti G. Objective assessment of the skin of children affected by atopic dermatitis: a study of pH, capacitance and TEWL in eczematous and clinically uninvolved skin. Acta Derm Venereol 1995;75:429-33.

46. Elias PM, Hatano Y, Williams ML. Basis for the barrier abnormality in atopic dermatitis: outside-inside-outside pathogenic mechanisms. J Allergy Clin Immunol 2008;121:1337-43.

47. Eberlein-Konig B, Schafer T, Huss-Marp J, Darsow U, Mohrenschlager M, Herbert O, et al. Skin surface pH, stratum corneum hydration, trans-epidermal water loss and skin roughness related to atopic eczema and skin dryness in a population of primary school children. Acta Derm Venereol 2000;80:188-91.

48. Nemoto-Hasebe I, Akiyama M, Nomura T, Sandilands A, McLean WH, Shimizu H. Clinical severity correlates with impaired barrier in filaggrin-related eczema. J Invest Dermatol 2009;129:682-9.

49. Hubiche T, Ged C, Benard A, Leaute-Labreze C, McElreavey K, de Verneuil H, et al. Analysis of SPINK 5, KLK 7 and FLG genotypes in a French atopic dermatitis cohort. Acta Derm Venereol 2007;87:499-505.
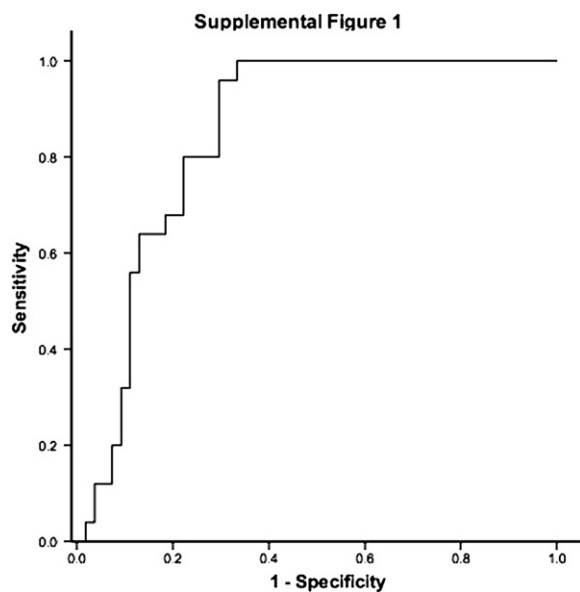
FIG E1. ROC curve for NMF values to distinguish $FLG^{+/-}$ subjects from $FLG^{-/-}$ subjects in the AD_{FLG} group. AUC is 0.85 (95% CI, 0.76-0.93), with a sensitivity of 96% and a specificity of 66.77% at a cutoff of 0.767 arbitrary units.